[16] J. T. Johnson, J. V. Toporkov, and G. S. Brown, "A numerical study of backscattering from time evolving sea surfaces: Comparison of hydrodynamic models," IEEE Trans. Geosci. Remote Sensing, to be published.
[17] J. V. Toporkov and G. S. Brown, "Numerical simulations of scattering from time-varying, randomly rough surfaces," *IEEE Trans. Geosci. Remote Sensing*, vol. 38, pp. 1616–1625, July 2000.
[18] R. F. Harrington, *Field Computation by Moment Method*. New York: IEEE Press, 1993.
[19] D. Torrungrueng and E. H. Newman, "The multiple sweep method of moments (MSMM) analysis of electrically large bodies," *IEEE Trans. Antennas Propagat.*, vol. 45, pp. 1252–1258, Aug. 1997.
[20] L. Tsang, J. A. Kong, and R. T. Shin, *Theory of Microwave Remote Sensing*. New York: Wiley, 1985.
[21] W. J. Plant, "The modulation transfer function: Concept and applications," in *Radar Scattering from Modulated Wind Waves*, G. J. Komen and W. A. Oost, Eds. Norwell, MA: Kluwer, 1989, pp. 155–172.
[22] D. Colak, R. J. Burkholder, and E. H. Newman, "The multiple sweep method of moments (MSMM) analysis of electromagnetic scattering from targets on ocean-like rough surfaces," *IEEE Trans. Geosci. Remote Sensing*, to be published.

A New Measurement Technique for Obtaining the Complex Relative Permittivity of Terrain Surfaces

Heung-Soo Kim and Ram M. Narayanan

***Abstract*—A new method for measuring the effective complex relative permittivity of a reflecting surface is presented. The approach is based on the two-ray model. We derive an equation of a circle representing the complex reflection coefficient which relates the incidence angle, frequency, and received power from the path gain using the two-ray model. The intersection point of three such circles at different heights, while maintaining the same incidence angle, yields the correct complex reflection coefficient value. By measuring the received power for both the vertical and horizontal polarizations, the relative permittivity of the surface can be determined. The technique is validated using computer simulation, as well as field measurements of typical terrain surfaces, such as asphalt, grass, and bare soil. A major advantage of this method is that it obviates the need to use antennas with a narrow beam pattern.**

***Index Terms*—Complex relative permittivity, reflection coefficient.**

I. Introduction

For radio and wireless systems operating over the earth's surface, it is necessary to characterize the radio frequency (RF) propagation channel for their proper installation and maintenance. Recently, there has been strong interest in ray-tracing techniques for propagation prediction [1]–[14]. In the case of the two-ray multipath propagation model, knowledge of the reflection coefficient of the ground surface is essential. Since it is difficult to accurately model these coefficients, many measurements have been made in order to obtain the range of values for these reflection coefficients, and from them the relative permittivities of the terrain surfaces. Typical values for the range of reflection coefficients of these surfaces are provided in [8] and [15]. One of the measurement methods described is a two-step technique [8]. The first step in this technique is to measure line-of-sight (LOS) channel impulse responses with the two narrow beamwidth antennas facing each other. Then, the antennas are aimed at the reflection point on the test surface, and reflected channel impulse responses are measured. In this technique, the transmitter and receiver locations are constrained by a number of factors, and the antennas used in the measurement are required to possess a sharp and narrow beam pattern.

In this communication, we present a simpler method to measure the reflection coefficients and thereby the effective complex relative permittivities of reflecting terrain surfaces. The equation of a circle is derived from the path gain of the two-ray model. By measuring the received power for different antenna heights at the same incidence angle at the frequency of interest, it is shown that the intersection of these circles occurs at the correct reflection coefficient of the surface under investigation. From these reflection coefficients, the complex relative permittivities can be obtained easily. One of the advantages of this method is that a broad beamwidth antenna can be used for the measurement. The relative permittivities of grass, asphalt, and soil surface are measured and presented using this method.

This communication is organized as follows. Section II provides the theoretical underpinnings of the technique developed for measuring the terrain surface reflection coefficients, and then calculating the complex relative permittivities. In Section III, we present simulation results (assuming a smooth surface) that demonstrate the validity of the analytical approach. In Section IV, we present field measurements on electromagnetically smooth terrain surfaces. Finally, Conclusions and summaries are given in Section V.

II. Two-Ray Model Above A Flat Surface

Consider a transmitter (T) located at a height h_T and a receiver (R) located at height h_R above the earth's surface. Let the distance between the transmitter and receiver be d, and the incidence angle at the earth reflection point be θ, as shown in Fig. 1. The transmitter sends out a spherical wave that is reflected from the ground and picked up by the receiver. In addition, the directly propagating wave is also picked up by the receiving antenna. We assume that the spherical wave travels along a family of radial lines, called *rays*, emanating from the transmitter. The distance between the transmitter and the receiver is r_1 along the direct path and r_2 along the reflected path.

The total received power at each polarization, due to the fields arriving along the direct and reflected ray paths can be shown as

$$P_R = \frac{P_T G_T G_R}{L}\left(\frac{\lambda}{4\pi}\right)^2 \cdot \left|\frac{1}{r_1}e^{-jkr_1} + \sqrt{\alpha_T}\cdot\sqrt{\alpha_R}\cdot\rho_{h,v}\frac{1}{r_2}e^{-jkr_2}\right|^2 \quad (1)$$

where

P_R	received power;
P_T	transmitted power;
G_T	transmit antenna power gain;
G_R	receive antenna power gain;
L	factor representing power loss in the cables and connectors;
λ	wavelength;
α_T and α_R	magnitude ratios of power patterns along the reflected to the direct path directions for the transmit and the receive antenna, respectively;
$\rho_{h,v}$	reflection coefficient of the ground, where subscripts h and v denote horizontal and vertical polarizations, respectively.

Manuscript received March 2, 2001; revised January 22, 2002.

H.-S. Kim is with the Faculty of Telecommunication and Computer Engineering, Cheju National University, Cheju 690-756, Korea.

R. M. Narayanan is with the Department of Electrical Engineering, Center for Electro-Optics, University of Nebraska, Lincoln, NE 68588-0511 USA.

Publisher Item Identifier S 0196-2892(02)04808-8.

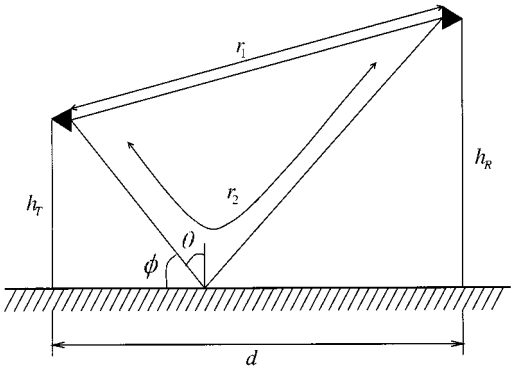

Fig. 1. Two-ray model for propagation above a flat surface.

If the ground has finite conductivity, its relative permittivity will be complex, and its reflection coefficient is given by

$$\rho_{h,v} = \Upsilon_{h,v} + j\zeta_{h,v} \tag{2}$$

where $\Upsilon_{h,v}$ and $\zeta_{h,v}$ are real and imaginary parts of the reflection coefficient, respectively. From (1) and (2), we can derive the equation of a circle on the complex reflection coefficient plane as

$$\left(\Upsilon_{h,v} + \frac{r_r \cos kr_d}{\sqrt{\alpha_T}\cdot\sqrt{\alpha_R}}\right)^2 + \left(\zeta_{h,v} + \frac{r_r \sin kr_d}{\sqrt{\alpha_T}\cdot\sqrt{\alpha_R}}\right)^2 = \left(\frac{4\pi r_2\sqrt{P_d}}{\lambda\cdot\sqrt{\alpha_T}\cdot\sqrt{\alpha_R}}\right)^2 \tag{3}$$

where

$$r_r = \frac{r_2}{r_1} \tag{4}$$

$$r_d = r_2 - r_1 \tag{5}$$

and

$$P_d = \frac{P_R L}{P_T G_T G_R}. \tag{6}$$

The center point of the circle is $\{-r_r \cos kr_d/(\sqrt{\alpha_T}\cdot\sqrt{\alpha_R}), -r_r \sin kr_d/(\sqrt{\alpha_T}\cdot\sqrt{\alpha_R})\}$, and its radius is $\{4\pi r_2\sqrt{P_d}/(\lambda\cdot\sqrt{\alpha_T}\cdot\sqrt{\alpha_R})\}$. The radius and the center of the circle depend on the heights of and distance between both antennas as well as the frequency. If these parameters are fixed, then the center point is fixed. However, the radius of the circle varies with the received power. The received power is dependent upon the surface reflection coefficient, and thus on its complex relative permittivity.

We can obtain the radius and center of the circle for a certain frequency by measuring the received power, the distance between the transmit and receive antennas, and their heights above the ground. Thereby, we can also determine the relative permittivity and the conductivity of the terrain surface by obtaining the reflection coefficients for both vertical and horizontal polarizations.

The circumference of the circles described in (3) contains the information on the reflection coefficients and represents the locus of all points that satisfy the equation. In order to uniquely obtain the reflection coefficient of the surface for each polarization, at least three such circles, from three separate measurements, are needed. This is due to the fact that while two circles will intersect at two points, three circles will intersect at only one point, representing the actual reflection coefficient. The reflection coefficients for both horizontal and vertical polarizations are given by

$$\rho_h = \frac{\sin\phi - \sqrt{\left(\frac{\varepsilon}{\varepsilon_0} + \frac{\sigma}{j\omega\varepsilon_0}\right) - \cos^2\phi}}{\sin\phi + \sqrt{\left(\frac{\varepsilon}{\varepsilon_0} + \frac{\sigma}{j\omega\varepsilon_0}\right) - \cos^2\phi}} \tag{7}$$

and

$$\rho_v = \frac{\left(\frac{\varepsilon}{\varepsilon_0} + \frac{\sigma}{j\omega\varepsilon_0}\right)\sin\phi - \sqrt{\left(\frac{\varepsilon}{\varepsilon_0} + \frac{\sigma}{j\omega\varepsilon_0}\right) - \cos^2\phi}}{\left(\frac{\varepsilon}{\varepsilon_0} + \frac{\sigma}{j\omega\varepsilon_0}\right)\sin\phi + \sqrt{\left(\frac{\varepsilon}{\varepsilon_0} + \frac{\sigma}{j\omega\varepsilon_0}\right) - \cos^2\phi}} \tag{8}$$

where

ϕ $(=90^\circ - \theta)$	grazing angle;
ε_0	permittivity of free space;
ε	permittivity of the surface;
σ	conductivity of the surface;
ω	angular frequency.

For the case of identical incidence angles for both polarizations, (7) and (8) yield the following relationship between those coefficients and complex relative permittivity ε_c, where $\varepsilon_r (=\varepsilon/\varepsilon_0)$ is the real part of the relative permittivity, and λ is the operating wavelength

$$\varepsilon_c = \varepsilon_r - j60\sigma\lambda = \frac{(1+\rho_v)(1-\rho_h)}{(1+\rho_h)(1-\rho_v)}. \tag{9}$$

Once we compute ρ_v and ρ_h from the intersection point of the circles, we can obtain the complex relative permittivity using (9).

III. Simulation Results

In order to validate this method, simulation studies were conducted. These simulations assumed an electromagnetically smooth surface of relative permittivity real part $\varepsilon_r = 15$, and conductivity $\sigma = 0.005$ S/m.

As described previously, in order to obtain one unique intersection point for the circles, at least three separate circles are needed. We know that the reflection coefficients depend on the frequencies, incidence angles, and the complex relative permittivities of the material of the reflection surface. As our goal is to find a complex relative permittivity at a particular frequency, three circles should be obtained at the same frequency and incidence angle. If the frequency and the incidence angle are fixed, the circles represent the reflection coefficients of the surface at the specified frequency and angle. The intersection point of a family of circles at the same frequency and incidence angle yields the reflection coefficient of the assumed material. To fix the incidence angle, we should maintain same ratio obtained from the height of the antennas and the distance between the transmitting and the receiving antenna. In our simulation, the distances between two antennas are 15 m, 20 m, and 25 m, and the corresponding height of both antennas are 0.9 m, 1.2 m, and 1.5 m, respectively (see the geometry in Fig. 1). Hence, the incidence angle θ is 83.157° for all cases. The frequency is assumed to be 1.8 GHz, consistent with the third-generation wireless networks.

We calculate the received powers from (1) and (2) for these three cases. We also assume that half-wave dipole antennas are used for both the transmitter and the receiver with a gain of 2.15 dB (1.64). For this antenna, the factor $\alpha_{T,R}$ is 1.000 for horizontal polarization and 0.979 for vertical polarization. We also assume lossless conditions, i.e., $L = 1$.

From (3), the centers and radii of three circles are obtained and the intersection of three circles is found for both polarizations. The circumference of these three circles are seen to coincide at a single point, as predicted by the theory, which represents the actual reflection coefficient of the assumed material. Fig. 2 shows the circles for the horizontal and vertical polarizations.

In Fig. 2, the abscissa represents the real part of the reflection coefficient, while the ordinate represents the imaginary part. The coincident point for each polarization represents ρ_h and ρ_v, respectively. As the range for the reflection coefficients is $[-1, +1]$, the coincident point must lie within this range. The values of these points in Fig. 2 are shown in Table I, and it is seen that this is indeed the case. Using (9), the inverted results for the real part of the relative permittivity and the

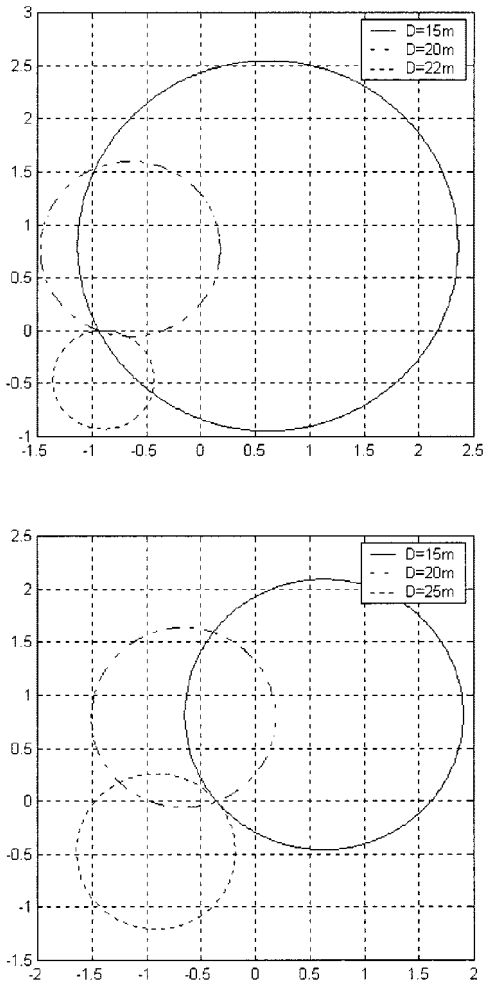

Fig. 2. Simulated complex reflection coefficient circles at different antenna separation distances for horizontal polarization (top) and vertical polarization (bottom).

TABLE I
RESULTS OF SIMULATION

Assumed Values	Real part of relative permittivity	15.000
	Conductivity	0.005 S/m
Intersection Point	Vertical Pol.	-0.3537 - j0.0007
	Horizontal Pol.	-0.9383 + j0.0001
Inverted Results	Real part of relative permittivity	15.000
	Conductivity	0.005 S/m

conductivity are 15.00 and 0.005 S/m, respectively. These values are the same as the assumed values, thereby validating our approach.

The circles should yield an intersection point for each polarization for the same surface. From the characteristics of the reflection coefficients, the intersection point for horizontal polarization should lie in the second quadrant, while the intersection point for vertical polarization should lie in the third or fourth quadrant; especially in the fourth quadrant when the incidence angle is smaller than the Brewster angle.

IV. MEASUREMENT RESULTS

A. Description of Experimental Setup

We chose three measurement sites representing asphalt, grass, and bare soil for the reflection coefficient measurements. The chosen sites were flat and relatively homogeneous in appearance, and were electromagnetically smooth at the 1.8-GHz measurement frequency. The

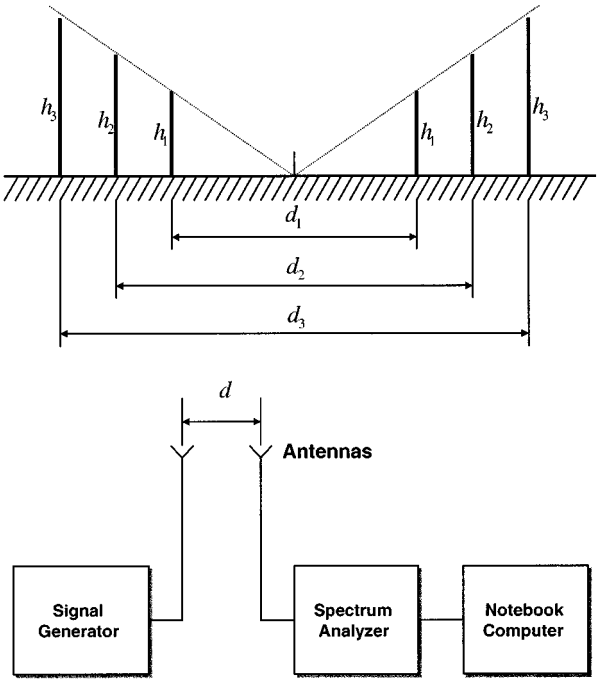

Fig. 3. Geometry of the experimental configuration.

TABLE II
SPECIFICATIONS OF THE MEASUREMENT SYSTEM

Antennas	Monopole		
Heights	1.08 m	1.2 m	1.32 m
Distances	18 m	20 m	22 m
Frequency	1.8 GHz		
Incidence Angle	83.157°		

criterion for a surface to be considered electromagnetically smooth is given as [16]

$$s < \frac{\lambda}{8 \sin \phi} \tag{10}$$

where

- s average roughness of the surface;
- λ wavelength;
- ϕ grazing angle.

The right-hand side of (10) is computed as 17.5 cm for $\lambda = 16.67$ cm and $\phi = 90° - 83.157° = 6.843°$. The maximum value of the actual surface roughness was about 6 cm, well below the value of 17.5 cm computed above. Thus, the surfaces could be considered to be electromatically smooth. Furthermore, the surfaces were relatively isolated from interfering objects which could induce additional reflection and scattering.

A pavement represented the asphalt surface. This was a road which had been paved many years ago. It was a long and straight abandoned road 18 m wide. There was nothing except electric poles on both sides of the road. The grass surface was a wide and flat area adjacent to the asphalt road. It also had no obstructions nearby. The bare soil surface was a corn field after harvesting, which contained some corn residue.

The geometry of the experimental configuration is illustrated in Fig. 3 with $h_T = h_R = h$ in all cases. The characteristics of the measurement geometry shown in Fig. 3 are presented in Table II.

Both antennas were identical monopoles the gain of which was measured as 3.4 dBi. Since the incidence angle was 83.157°, $\alpha_{T,R}$ of the antenna were determined to be 1.0000 and 0.9936, respectively. The

TABLE III
RESULTS OF MEASUREMENT FOR ASPHALT, GRASS, AND BARE SOIL

Geometry	Polarization	Transmitted power	Average received power (dBm)		
			Asphalt	Grass	Soil
d=18 m	Vertical	-10 dBm	-72.24	-72.33	-72.66
h=1.08 m	Horizontal	-10 dBm	-71.38	-70.89	-70.77
d=20 m	Vertical	-10 dBm	-75.52	-75.39	-73.67
h=1.2 m	Horizontal	-10 dBm	-76.20	-74.54	-75.30
d=22 m	Vertical	-10 dBm	-78.67	-79.06	-75.01
h=1.32 m	Horizontal	-10dBm	-83.48	-84.70	-84.26

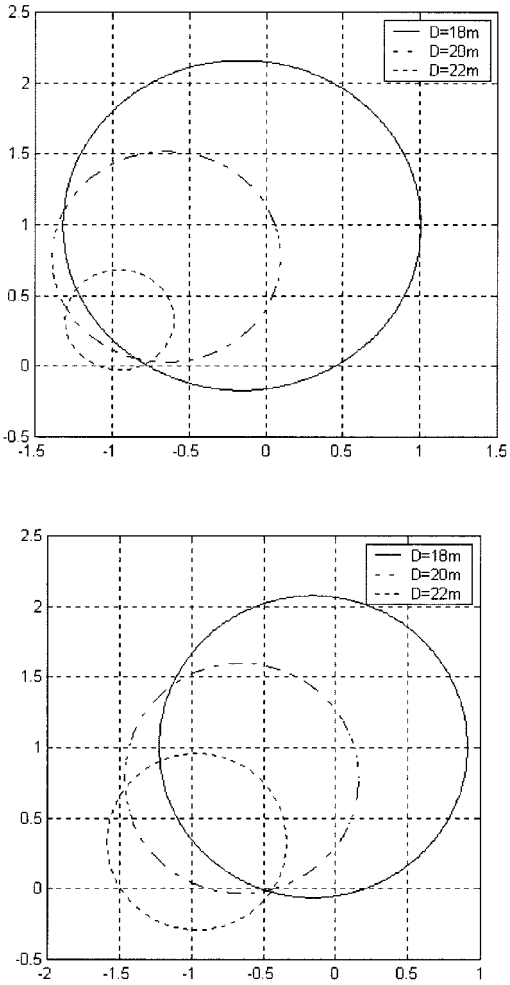

Fig. 4. Measured complex reflection coefficient circles for asphalt surface at different antenna separation distances for horizontal polarization (top) and vertical polarization (bottom).

total loss of the cable and connectors was measured to be 14.7 dB; thus $L = 29.51$.

The power transmitted was -10 dBm. At the receiver, the signals were received by a spectrum analyzer and the received power strength recorded using a notebook computer at a rate of 3 samples/s. A total of 300 data samples were collected for each experiment in order to reduce the effects of noise and measurement uncertainty.

B. Measurement Results and Analysis

The collected received data showed a standard deviation of less than 3 dB. These data were averaged to obtain the mean received power in each case. Since a total of 300 samples were incoherently averaged, the error in the averaged power measurement was computed as approximately 0.17 dB (~ 3 dB/$\sqrt{300}$). This translates to an error (± 1 standard deviation) of about 3.8% in P_d in (3). Thus, the error in the magnitude of the reflection coefficient is approximately one-half of the above, i.e., 1.9%. This error can be related to the error in the complex relative permittivity using (4) and (5), but the analysis is cumbersome. However, the above simple analysis provides confidence in the reduction in the error by averaging.

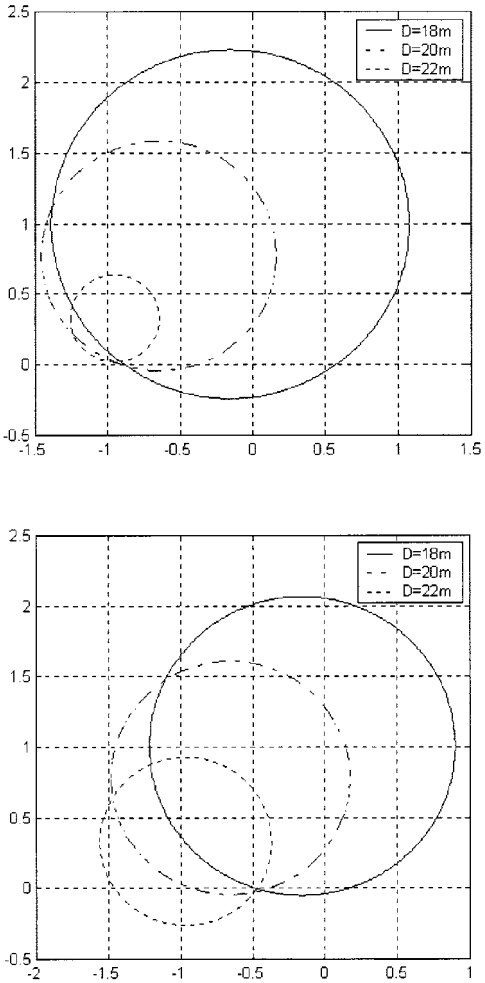

Fig. 5. Measured complex reflection coefficient circles for grass surface at different antenna separation distances for horizontal polarization (top) and vertical polarization (bottom).

Table III shows the average values of the received powers for the three surfaces. These values take into account the signal loss and the antenna gains.

Figs. 4–6 show the three circles for the asphalt, grass, and soil surface at both polarizations, respectively. From Figs. 4–6, we note that the circles do not exactly coincide at one unique point, although these are very close. We attribute this to experimental error. Thus, three intersection points are obtained in each case and averaged. The values of the coordinates of the individual intersection points are shown in Table IV. Using (9), the complex relative permittivities and the conductivities are easily obtained, and these are also shown in Table IV. These values fall within the range of expected values, and are indeed appropriate for the surfaces in question.

V. CONCLUSIONS

A new method for measuring the complex relative permittivity of reflecting surfaces has been proposed. This new method appears to be easier than other proposed methods, and may be used with antennas without narrow beam patterns. In addition, the technique avoids the

TABLE IV
INTERSECTION POINTS AND COMPLEX RELATIVE PERMITTIVITIES FOR ASPHALT, GRASS, AND BARE SOIL

Surface	Horizontal polarization	Vertical polarization	Relative permittivity	Conductivity
Asphalt	- 0.8470 + j0.0569	- 0.4776 - j0.0127	3.16 - j0.73	0.073 S/m
	-0.7880 + j0.0155	-0.4506 - j0.0207		
	-0.7533 + j0.0363	-0.4388 - j0.0031		
Grass	-0.9568 + j0.0217	-0.4915- j0.0281	8.09 - j1.63	0.163 S/m
	-0.9168 + j0.0236	-0.4341 - j0.0147		
	-0.8763 + j0.0068	-0.4759 - j0.0035		
Soil	-0.9518 + j0.0058	- 0.0981 - j0.0588	21.95 - j0.82	0.082 S/m
	-0.9232 + j0.0069	-0.0769 - j0.0083		
	-0.8945 + j0.0147	-0.0206 - j0.0022		

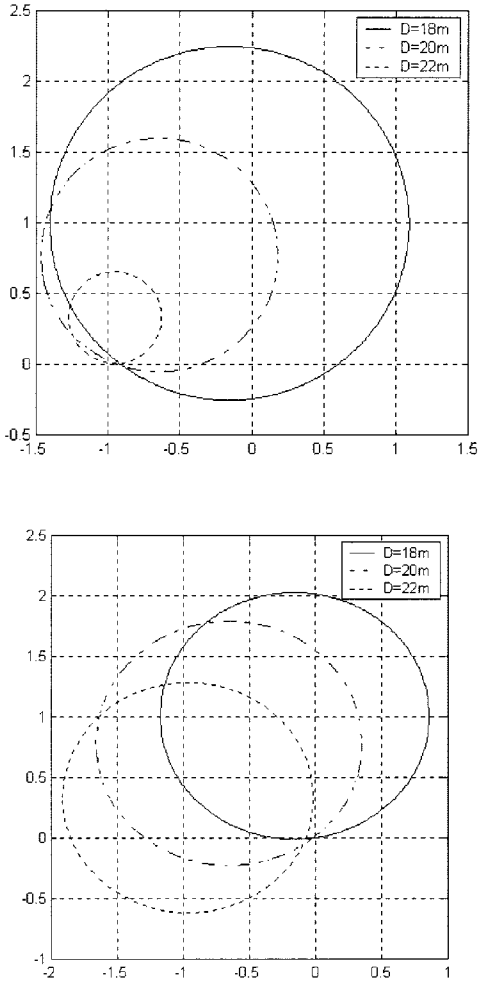

Fig. 6. Measured complex reflection coefficient circles for bare soil surface at different antenna separation distances for horizontal polarization (top) and vertical polarization (bottom).

use of expensive and sophisticated instrumentation. The relative permittivity of typical surfaces, such as asphalt, grass, and soil, have been obtained using this method, and the values obtained appear to be very reasonable and consistent with prior measurements [8], [15].

We would like to conclude with some comments. The technique makes use of the coherent superposition of the direct and the reflected signals from the terrain surface. The smooth surface reflection coefficient formulation is valid for surfaces that satisfy (10). If the surface is rough, the scattering will contain both specular (coherent) and diffuse (incoherent) components, and the amplitude of the specular component will depend also on the roughness of the terrain surface. In this case, the inversion of the complex relative permittivity will contain higher error.

ACKNOWLEDGMENT

The authors appreciate technical and logistic support provided by K. Atanassov.

REFERENCES

[1] T. S. Rappaport, "Characterization of UHF multipath radio channels in factory buildings," *IEEE Trans. Antennas Propagat.*, vol. 37, pp. 1058–1069, Aug. 1989.
[2] J. F. Lafortune and M. Lecours, "Measurement and modeling of propagation losses in a building at 900 MHz," *IEEE Trans. Veh. Technol.*, vol. 39, pp. 101–108, May 1990.
[3] F. Ikegami, T. Takeuchi, and S. Yoshida, "Theoretical prediction of mean field strength for urban mobile radio," *IEEE Trans. Antennas Propagat.*, vol. 39, pp. 299–302, Mar. 1991.
[4] S. Y. Seidel and T. S. Rappaport, "914 MHz path loss prediction models for indoor wireless communications in multifloored buildings," *IEEE Trans. Antennas Propagat.*, vol. 50, pp. 207–217, Feb. 1992.
[5] N. Amitay, "Modeling and computer simulation of wave propagation in lineal line-of-sight microcells," *IEEE Trans. Veh. Technol.*, vol. 41, pp. 337–342, Nov. 1992.
[6] O. Landron, M. J. Feuerstein, and T. S. Rappaport, "*In-situ* microwave reflection coefficient measurements for smooth and rough exterior wall surfaces," in *Proc. 43rd IEEE VTC*, Secaucus, NJ, May 1993, pp. 77–80.
[7] S. Jenvey, "Ray optics modeling for indoor propagation at 1.8 GHz," in *Proc. 44th IEEE VTC*, Stockholm, Sweden, June 1994, pp. 1750–1753.
[8] V. Erceg, A. J. Rustako, and R. S. Roman, "Diffraction around corners and its effects on the microcell coverage area in urban and suburban environment at 900 MHz, 2 GHz, and 6 GHz," *IEEE Trans. Veh. Technol.*, vol. 43, pp. 762–766, Aug. 1994.
[9] S. Y. Seidel and T. S. Rappaport, "Site-specific propagation prediction for wireless in-building personal communication system design," *IEEE Trans. Veh. Technol.*, vol. 43, pp. 879–891, Nov. 1994.
[10] M. C. Lawton and J. P. McGeehan, "The application of a deterministic ray launching algorithm for the prediction of radio channel characteristics in small-cell environments," *IEEE Trans. Veh. Technol.*, vol. 43, pp. 955–969, Nov. 1994.
[11] O. Landron, M. J. Feuerstein, and T. S. Rappaport, "A comparison of theoretical and empirical reflection coefficients for typical exterior wall surfaces in a mobile radio environment," *IEEE Trans. Antennas Propagat.*, vol. 44, pp. 341–351, Mar. 1996.
[12] P. F. M. Smulders and L. H. Correia, "Characterization of propagation in 60 GHz radio channels," *Electron. Commun. Eng. J.*, vol. 9, pp. 73–80, Apr. 1997.
[13] K. W. Cheung, J. H. M. Sau, and R. D. Murch, "A new empirical model for indoor propagation prediction," *IEEE Trans. Veh. Technol.*, vol. 47, pp. 996–1001, Aug. 1998.
[14] W. C. Y. Lee, *Mobile Cellular Telecommunication Systems*. New York: McGraw-Hill, 1989.
[15] H. L. Bertoni, *Radio Propagation for Modern Wireless Systems*. Englewood Cliffs, NJ: Prentice-Hall, 2000.
[16] N. Blaunstein, *Radio Propagation in Cellular Networks*. Norwood, MA: Artech House, 2000.